Physics Letters B 734 (2014) 383–387

Contents lists available at ScienceDirect

Physics Letters B

www.elsevier.com/locate/physletb

Constraining hypernuclear density functional with Λ-hypernuclei and compact stars

E.N.E. van Dalen [a], G. Colucci [b], A. Sedrakian [b,*]

[a] Institute for Theoretical Physics, Tübingen University, D-72076 Tübingen, Germany
[b] Institute for Theoretical Physics, J.-W. Goethe University, D-60438 Frankfurt am Main, Germany

ARTICLE INFO

Article history:
Received 30 April 2014
Accepted 2 June 2014
Available online 5 June 2014
Editor: W. Haxton

Keywords:
Neutron stars
Hypernuclei
Equations of state: nuclear matter

ABSTRACT

We present a simultaneous calculation of heavy single-Λ hypernuclei and compact stars containing hypernuclear core within a relativistic density functional theory based on a Lagrangian which includes the hyperon octet and lightest isoscalar-isovector mesons which couple to baryons with density-dependent couplings. The corresponding density functional allows for SU(6) symmetry breaking and mixing in the isoscalar sector, whereby the departures in the $\sigma-\Lambda$ and $\sigma-\Sigma$ couplings away from their values implied by the SU(3) symmetric model are used to adjust the theory to the laboratory and astronomical data. We fix $\sigma-\Lambda$ coupling using the data on the single-Λ hypernuclei and derive an upper bound on the $\sigma-\Sigma$ from the requirement that the lower bound on the maximum mass of a compact star is $2M_{\odot}$.

1. Introduction

The current and upcoming experimental studies of the properties of Λ-hypernuclei in laboratory, such as HKS experiment at JLab in the US, J-PARC experiment in Japan, PANDA experiment at FAIR in Germany, the ALICE experiment at CERN, will greatly advance our understanding of the strange sector of the nuclear forces and properties of hypernuclei. Astronomical motivation to study hypernuclear stars resurged after the recent observations of two-solar-mass pulsars in binary orbits with white dwarfs [1,2]. Hyperons become energetically favorable once the Fermi energy of neutrons exceeds their rest mass. The onset of hyperons reduces the degeneracy pressure of a cold thermodynamic ensemble, therefore, the equation of state (EoS) becomes softer than in the absence of the hyperons. As a result the maximum possible mass of a compact star decreases to values which contradict the observations. This contradiction is known as "hyperonization puzzle".

What can be said about the effective amount of attraction of hypernuclear forces? The experimental observations of bound Λ-hypernuclei imply that the interaction must be attractive enough to bind a Λ particle to a medium and heavy mass nucleus. At the same time the existence of two-solar-mass pulsars requires sufficient repulsion (at least at high densities) to guarantee the stability of hypernuclear compact stars, if such exist. Therefore, *the combined laboratory and astronomical data limit from above and below the attraction among hyperons in nuclear medium in any particular model.*

In this work we use a relativistic density functional theory (DFT) of hypernuclear matter to extract these bounds. Density functional theory is a very successful theoretical tool to study complex many-body systems in various fields including strongly correlated electronic systems, quantum chemistry, atomic and molecular systems, classical liquids, magnetic materials, etc. [3]. In particular, relativistic covariant DFTs have been applied to study bulk hypernuclear systems and compact stars both in the past (see, for example, [4,5] for an account of the early work) and in recent years, notably to address the "hyperonization puzzle" [6–14]. Glendenning and Moszkowski [15] were the first to recognize the importance of reconciliation of neutron-star masses and binding energies of the Λ-hypernuclei. Since the recent discoveries of heavy compact stars the astronomical constraints have become much tighter. The quality of relativistic density functionals have considerably improved in the last decade due to better constraints from the phenomenology of nuclei [16]. Here we use an extension of nuclear density functional with a density-dependent parameterization of the couplings [16], which was extended to the hypernuclear sector in Ref. [17] within the SU(3) symmetric model. The focus of that work was on the sensitivity of the EoS of hypernuclear matter to the unknown hyperon–scalar-meson couplings. Within this framework, it was argued that the parameters can be tuned such that two-solar mass hyperonic compact stars emerge (which is not possible within the standard SU(3) parameterization).

* Corresponding author.
E-mail addresses: eric.van-dalen@uni-tuebingen.de (E.N.E. van Dalen), colucci@th.physik.uni-frankfurt.de (G. Colucci), sedrakian@th.physik.uni-frankfurt.de (A. Sedrakian).

http://dx.doi.org/10.1016/j.physletb.2014.06.002

Here we test this model by carrying out calculations of a number of hypernuclei and by providing a *combined constraint* on the parameters of the underlying DFT by invoking both the astronomical and laboratory data on hypernuclear systems. We show that the coupling of σ-meson to the Λ-hyperon can be optimized to fit the data on hypernuclei, thus narrowing down the parameter space. We then constrain the parameter space of the remaining σ–Σ coupling using some general inequalities as well as astronomical observations of the $2M_\odot$ pulsars.

2. Density functional theory of hypernuclear matter

The relativistic Lagrangian density of our model reads

$$\begin{aligned}\mathcal{L} = \sum_B \bar{\psi}_B \Big[\gamma^\mu \Big(i\partial_\mu - g_{\omega B}\omega_\mu - \frac{1}{2} g_{\rho B} \boldsymbol{\tau}\cdot\boldsymbol{\rho}_\mu \Big) \\ - (m_B - g_{\sigma B}\sigma) \Big] \psi_B + \frac{1}{2}\partial^\mu\sigma\,\partial_\mu\sigma - \frac{m_\sigma^2}{2}\sigma^2 \\ - \frac{1}{4}\omega^{\mu\nu}\omega_{\mu\nu} + \frac{m_\omega^2}{2}\omega^\mu\omega_\mu - \frac{1}{4}\boldsymbol{\rho}^{\mu\nu}\boldsymbol{\rho}_{\mu\nu} \\ + \frac{m_\rho^2}{2}\boldsymbol{\rho}^\mu\cdot\boldsymbol{\rho}_\mu + \sum_\lambda \bar{\psi}_\lambda \big(i\gamma^\mu\partial_\mu - m_\lambda \big)\psi_\lambda, \end{aligned} \tag{1}$$

where the B-sum is over the $J^P = \frac{1}{2}^+$ baryon octet, ψ_B are the baryonic Dirac fields with masses m_B. The meson fields σ, ω_μ and $\boldsymbol{\rho}_\mu$ mediate the interaction among baryon fields, $\omega_{\mu\nu}$ and $\boldsymbol{\rho}_{\mu\nu}$ represent the field strength tensors of vector mesons and m_σ, m_ω, and m_ρ are their masses. The baryon–meson coupling constants are denoted by g_{mB}. The last line of Eq. (1) stands for the contribution of the free leptons, where the λ-sum runs over the leptons e^-, μ^-, ν_e and ν_μ with masses m_λ. The density dependence of the couplings implicitly takes into account many-body correlations among nucleons which are beyond the mean-field approximation. The nucleon–meson coupling constants are parametrized as $g_{iN}(\rho_B) = g_{iN}(\rho_0)h_i(x)$, for $i = \sigma, \omega$, and $g_{\rho N}(\rho_B) = g_{\rho N}(\rho_0)\exp[-a_\rho(x-1)]$ for the $\boldsymbol{\rho}_\mu$-meson, where ρ_B is the baryon density, ρ_0 is the saturation density, $x = \rho_B/\rho_0$ and the explicit form of the functions $h_i(x)$ and the values of couplings can be found elsewhere [16,17]. This density functional is consistent with the following parameters of nuclear systems: saturation density $\rho_0 = 0.152$ fm^{-3}, binding energy per nucleon $E/A = -16.14$ MeV, incompressibility $K_0 = 250.90$ MeV, symmetry energy $J = 32.30$ MeV, symmetry energy slope $L = 51.24$ MeV, and symmetry incompressibility $K_{\rm sym} = -87.19$ MeV all taken at saturation density [18]. These values of parameters are in an excellent agreement with the nuclear phenomenology [19]. The third order derivatives of the energy and symmetry energy with respect to density taken at saturation have the following values $Q_0 = 478.30$ and $Q_{\rm sym} = 777.10$ MeV.

The pressure and energy density of the model is further supplemented by the contribution coming from the so-called rearrangement self-energy [20,21], which guarantees the thermodynamical consistency. The hyperon–meson couplings are fixed according to the SU(3)-flavor symmetric octet model. Due to the universal coupling of the $\boldsymbol{\rho}_\mu$ meson to the isospin current and the ideal mixing between the ω and ϕ mesons [22], the couplings between hyperons and vector mesons are as follows:

$$\begin{aligned} &x_{\rho\Xi} = 1, \qquad x_{\rho\Sigma} = 2, \qquad x_{\omega\Xi} = \frac{1}{3}, \\ &x_{\omega\Sigma} = x_{\omega\Lambda} = \frac{2}{3}, \qquad x_{\rho\Lambda} = 0, \end{aligned} \tag{2}$$

where $x_{\rho\Xi} = g_{\rho\Xi}/g_{\rho N}$, $x_{\rho\Sigma} = g_{\rho\Sigma}/g_{\rho N}$, etc.

Within the octet model the baryon–scalar-mesons couplings of the scalar octet can be expressed in terms of only two parameters, the nucleon–a_0-meson coupling constant g_S and the $F/(F+D)$ ratio of the scalar octet [23]. Allowing for mixing of the scalar singlet state, the couplings of the baryons with the σ-meson obey the following relation [17]: $2(g_{\sigma N} + g_{\sigma\Xi}) = 3g_{\sigma\Lambda} + g_{\sigma\Sigma}$. We assume that the hyperon coupling constants must be positive and less than the nucleon coupling constants. Solving this equation for one of the dependent hyperon–σ-meson coupling constant, say $g_{\sigma\Xi}$, one finds

$$1 \le \frac{1}{2}(3x_{\sigma\Lambda} + x_{\sigma\Sigma}) \le 2. \tag{3}$$

These inequalities define a bound on the area spanned by the coupling constants $x_{\sigma\Lambda}$ and $x_{\sigma\Sigma}$, which we will constrain further in the following.

3. Finite nuclei

We now apply the same density functional, which is derived from the Lagrangian (1) to finite Λ-nuclei. For alternative applications of relativistic density functionals to finite Λ-hypernuclei see, for example, Refs. [24–26] and references therein. The Hamiltonian for protons, neutrons, and Λ-hyperons is the sum of the nuclear Hartree–Fock (HF) part and the Coulomb contribution which acts only among the charged particles (here protons)

$$H_{\rm HF,B} = H_{\rm RMF,B} + H_{\rm Coul}\delta_{Bp}, \tag{4}$$

where $H_{\rm RMF,B}$ is the mean-field Hamiltonian corresponding to the density functional discussed above and $H_{\rm Coul}$ denotes the Coulomb contribution. Note that the Hamiltonian is local. It is defined in terms of the single-particle densities resulting from the eigenstates of $H_{\rm HF,B}$, which implies that they have to be determined in a self-consistent way. The HF Hamiltonian is expressed in terms of the matrix elements between the basis states $\langle\alpha|H_{\rm HF,B}|\beta\rangle$ of an appropriate basis. The HF single-particle states $|\Psi_n\rangle$ are defined in terms of the expansion coefficients in this basis

$$|\Psi_n\rangle = \sum_\alpha |\alpha\rangle\langle\alpha|\Psi_n\rangle = \sum_\alpha c_{n\alpha}|\alpha\rangle. \tag{5}$$

If the HF variational procedure is constrained to a spherical description of hypernuclei, an appropriate basis system is formed by spherical plane wave basis [27,28], where a baryon is freely moving in a spherical cavity with a radius R. Since the HF Hamiltonian is already diagonal in the angular momentum quantum numbers j, l, and m, it only needs to be diagonalized in the radial quantum number. The radial part of the wave function is then expanded in terms of spherical Bessel functions. The radius R is chosen to be large enough to guarantee that the results for the bound single-particle states are insensitive to the changes in the value of R. Furthermore, we choose the number of basis states high enough to guarantee that the results are not affected by the truncation. The eigenvalues, i.e. the single-particle energies, and eigenvectors, i.e. the expansion coefficients, are then determined by matrix diagonalizations of the Hamiltonians for the protons, neutrons, and Λ-hyperons.

The total energy of a Λ-hypernucleus $E_{\rm tot}$ can then be obtained from the expression,

$$E_{\rm tot} = \frac{1}{2}\sum_{\alpha,B}\eta_\alpha^B\big(t_\alpha^B + \varepsilon_\alpha^B\big) + E_{\rm rear} + E_{\rm cm}, \tag{6}$$

where ε_α^B is the single-particle energy of the B-baryon, t_α^B is its kinetic energy, and η_α^B is its occupation factor. Because the couplings of our model are density-dependent we need to include

Table 1
Properties of Λ-hypernuclei $^{17}_{\Lambda}$O, $^{41}_{\Lambda}$C, and $^{49}_{\Lambda}$C for the models *a*, *b*, and *c*. The columns list the single-particle energy of the Λ $1s_{1/2}$ state, the binding energy and the rms radii for neutrons, protons and Λ-hyperon.

	Λ $1s_{1/2}$ state [MeV]	E/A [MeV]	r_p [fm]	r_n [fm]	r_Λ [fm]
$^{17}_{\Lambda}$O					
a	0.846	−7.443	2.609	2.579	8.313
b	−4.564	−7.760	2.606	2.576	3.203
c	−27.279	−9.035	2.563	2.534	1.977
$^{41}_{\Lambda}$C					
a	0.934	−8.336	3.372	3.319	8.710
b	−8.519	−8.565	3.370	3.317	3.168
c	−35.224	−9.199	3.347	3.294	2.298
$^{49}_{\Lambda}$C					
a	0.973	−8.442	3.389	3.576	8.825
b	−9.882	−8.662	3.387	3.571	3.140
c	−37.257	−9.207	3.365	3.548	2.419

the rearrangement contribution $E_{\rm rear}$ to insure the consistency of the model. Finally, the center of mass correction is given by $E_{\rm cm} = -(1/2M)\langle \boldsymbol{P}^2_{\rm cm}\rangle$, with

$$\langle \boldsymbol{P}^2_{\rm cm}\rangle = \sum_\alpha \eta_\alpha \langle\alpha|\boldsymbol{p}^2_\alpha|\alpha\rangle - \sum_{\alpha\beta}(\eta_\alpha\eta_\beta + \zeta_\alpha\zeta_\beta)\langle\beta|\boldsymbol{p}_\alpha|\alpha\rangle\cdot\langle\alpha|\boldsymbol{p}_\beta|\beta\rangle, \quad (7)$$

where ζ_α is the anomalous occupation factor. To explore the sensitivity of the results on the coupling of Λ-hyperon to mesons we consider three sets of parameters: model *a* with $x_{\sigma\Lambda} = 0.52$, model *b* with $x_{\sigma\Lambda} = 0.59$, and model *c* with $x_{\sigma\Lambda} = 0.66$; all three models have $x_{\omega\Lambda} = 2/3$ and $x_{\rho\Lambda} = 0$. The HF calculations were carried out in a spherical box with a radius of $R = 15$ fm using the spherical plane wave basis for the Λ-hypernuclei $^{17}_{\Lambda}$O, $^{41}_{\Lambda}$Ca, and $^{49}_{\Lambda}$Ca. The results of these calculations are presented in Table 1, where we list the single-particle energy of the Λ $1s_{1/2}$ state, the binding energy of the nucleus and the rms radii r_B for neutrons, protons and the Λ-hyperon. Model *a* with the smallest value of the Λ–σ coupling predicts a positive single-particle energy for the Λ $1s_{1/2}$ state of these nuclei, which means that the Λ-hyperon is not bound. The fact that one does not have a hypernucleus is also reflected in the unusually large value of r_Λ. The other two models with larger values of the Λ–σ coupling predict negative single-particle energies of the Λ $1s_{1/2}$ state. It is seen from Table 1 that a larger value of the Λ–σ coupling yields a larger binding energy and a smaller r_Λ.

In Fig. 1 we show the proton, neutron, and Λ density distributions in $^{49}_{\Lambda}$Ca. Since model *a* with its smallest value of the Λ–σ coupling clearly contradicts experimental data, only models *b* and *c* are considered. The model *c* which has the largest value of the Λ–σ coupling predicts the highest central Λ density for $^{49}_{\Lambda}$Ca. Also the neutron and proton density distributions are to some extent affected by the large value of the Λ–σ coupling.

Table 1 shows clearly that the single-particle energy of the Λ $1s_{1/2}$ state is very sensitive to the value of the Λ–σ coupling. The experimental data on properties of a number of Λ-hypernuclei, such as the single-particle energy of the Λ $1s_{1/2}$ state, has been used to construct a mass formula [29], which extends the familiar Bethe–Weizsäcker mass formula to include in addition to the non-strange nuclei the Λ-hypernuclei. A comparison with the predictions of this mass formula shows that the Λ $1s_{1/2}$ states in the model *b* are too weakly bound, whereas those in the model *c* are too strongly bound. Therefore, we proceed further to fine-tune the $x_{\sigma\Lambda}$ coupling in order to fit the values of the single-particle energies, i.e. separation energies of the Λ particle, obtained from the

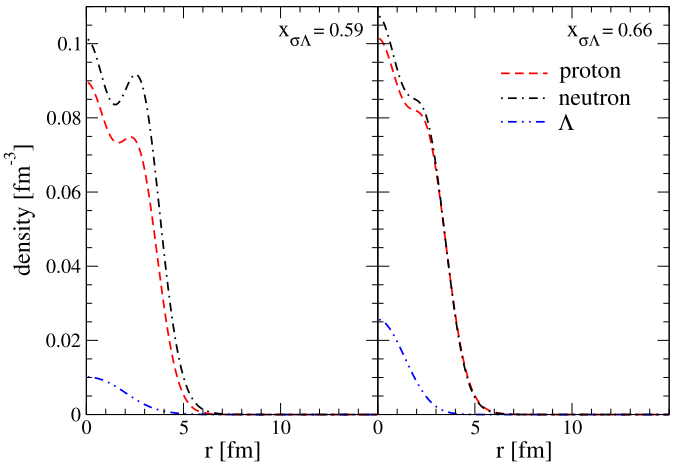

Fig. 1. (Color online.) Proton (dashed), neutron (dashed–dotted), and Λ (dashed–double dotted) density distributions in $^{49}_{\Lambda}$C for the models *b* (left panel) and *c* (right panel).

Table 2
Single-particle energies of the Λ $1s_{1/2}$ states, binding energies, and rms radii of the Λ-hyperon, neutron, and proton of $^{17}_{\Lambda}$O, $^{41}_{\Lambda}$C, and $^{49}_{\Lambda}$Ca are presented for optimal model. In addition, single-particle energies of the Λ $1s_{1/2}$ states, i.e. separation energies of the Λ-particle, obtained from the mass formula of Ref. [29] are given for these Λ-hypernuclei. Furthermore, the properties of ^{16}O, ^{40}Ca, and ^{48}Ca are given for the optimal model.

	$E_{\rm Mass}[\Lambda\ 1s_{1/2}]$ [MeV]	$E[\Lambda\ 1s_{1/2}]$ [MeV]	E/A [MeV]	r_p [fm]	r_n [fm]	r_Λ [fm]
$^{17}_{\Lambda}$O	−12.109	−11.716	−8.168	2.592	2.562	2.458
^{16}O	–	–	−8.001	2.609	2.579	–
$^{41}_{\Lambda}$C	−17.930	−17.821	−8.788	3.362	3.309	2.652
^{40}Ca	–	–	−8.573	3.372	3.320	–
$^{49}_{\Lambda}$Ca	−19.215	−19.618	−8.858	3.379	3.562	2.715
^{48}Ca	–	–	−8.641	3.389	3.576	–

mass formula of Ref. [29]. The *optimal model* obtained in this way has $x_{\sigma\Lambda} = 0.6164$. Within this optimal model we have recomputed the properties of $^{17}_{\Lambda}$O, $^{41}_{\Lambda}$Ca, and $^{49}_{\Lambda}$Ca. The results are given in Table 2, where we observe that the rms radius of the Λ in the $1s_{1/2}$ state increases with increasing mass number, which is in agreement with other theoretical models [24–26].

In Table 2, the properties of ^{16}O, ^{40}Ca, and ^{48}Ca are also given to investigate the effects of the Λ hyperon on the nucleons. The binding energies of $^{17}_{\Lambda}$O, $^{41}_{\Lambda}$Ca, and $^{49}_{\Lambda}$Ca are larger than those of ^{16}O, ^{40}Ca, and ^{48}Ca, respectively. This can be explained by the fact that the nucleon single-particle states are slightly deeper due to the presence of the Λ-hyperon. In addition, the rms radii of the nucleons are slightly smaller (by about 0.01 to 0.02 fm) in the Λ-hypernuclei. However, the addition of the Λ-hyperon to ^{16}O and ^{40}Ca does not change the differences between neutron and proton radii (neutron skin). The values of neutron skin in these nuclei are $r_n - r_p = -0.030$ and -0.052 fm, respectively. Only in the case of ^{48}Ca we observe a small change: the neutron skin changes from 0.187 fm in ^{48}Ca to 0.184 fm in $^{49}_{\Lambda}$Ca.

4. Compact stars

The recent observations of two-solar-mass pulsars in binary orbits with white dwarfs [1,2] place an observational lower bound on the maximum mass of any sequence of compact stars based on the unique equation of state (hereafter EoS) of dense matter. Massive compact stars may demand substantial population of heavy

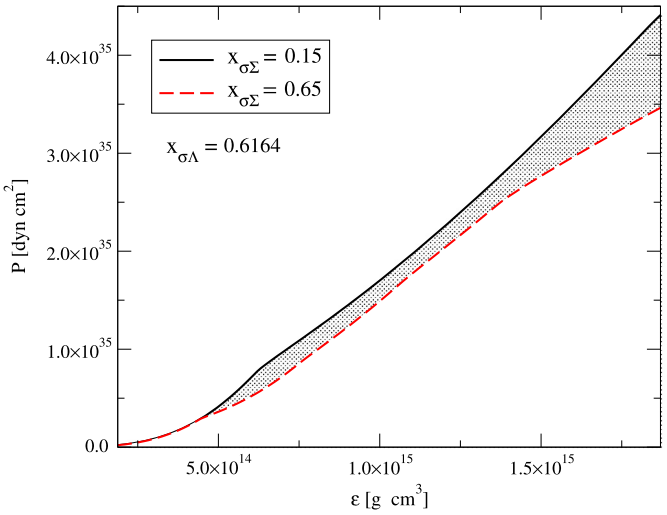

Fig. 2. (Color online.) Zero temperature equations of state of hypernuclear matter for fixed $x_{\sigma\Lambda} = 0.6164$ and a range of values $0.15 \leq x_{\sigma\Sigma} \leq 0.65$. These values generate the shaded area, which is bound from below by the softest EoS (dashed red line) corresponding to $x_{\sigma\Sigma} = 0.65$ and from above by the hardest EoS (solid line) corresponding to $x_{\sigma\Sigma} = 0.15$.

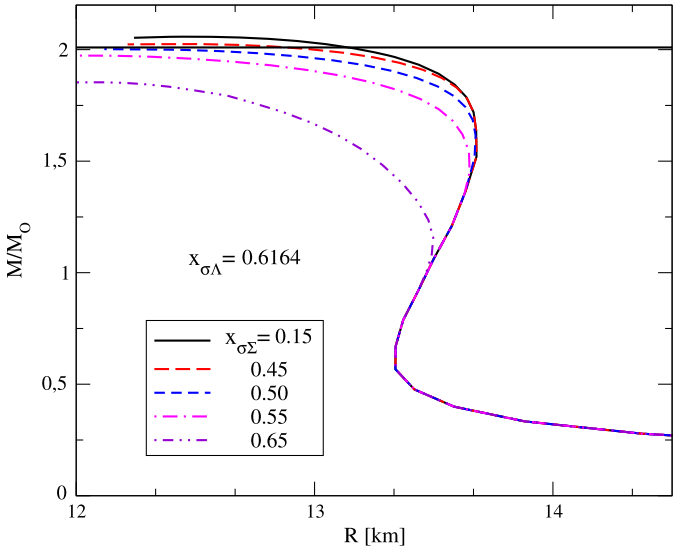

Fig. 3. (Color online.) The mass–radius relations for compact hypernuclear stars at zero temperature. We fix $x_{\sigma\Lambda} = 0.6164$ and assign values to $x_{\sigma\Sigma}$ from the range $0.15 \leq x_{\sigma\Sigma} \leq 0.65$ as indicated in the plot. The horizontal line shows the observational lower limit on the maximum mass $2.01(\pm 0.04) M_\odot$ [2].

baryons (hyperons). In Ref. [17] *both* parameters $x_{\sigma\Lambda}$ and $x_{\sigma\Lambda}$ were varied around the Nijmegen Soft Core (NSC) potential value $x_{\sigma\Lambda} = 0.58$ and $x_{\sigma\Sigma} = 0.448$ [30] in a range that is consistent with Eq. (3). In this section we revisit this problem using additional insight gained from the studies of the Λ-hypernuclei above. Specifically, we use the optimal model from previous section to fix the value $x_{\sigma\Lambda} = 0.6164$. Then, we are left with the coupling $g_{\sigma\Sigma}$ which is allowed to vary in the limits provided by Eq. (3).

The dependence of the EoS on the variation of the Σ–σ coupling at $T = 0$ at fixed value of Λ–σ is shown in Fig. 2. The stiffest EoS is obtained for the smallest value of $x_{\sigma\Sigma} = 0.15$. The EoS band generated by the values of $0.15 \leq x_{\sigma\Sigma} \leq 0.65$ is bounded from below by EoS which, as we shall see, is incompatible with the lower bound on the maximum mass of a compact star. Therefore, the parameter space included in this figure can be narrowed down further by exploring the masses of corresponding configurations. Fig. 3 shows the gravitational masses (in solar units) vs radii for our sequences of stars. First, we see that large enough masses can be obtained within the parameter range covered. However, for large enough $x_{\sigma\Sigma}$ the maximum masses of the sequences drop below the observational value $2M_\odot$, specifically for $x_{\sigma\Lambda} = 0.6164$ this occurs for $x_{\sigma\Sigma} \geq 0.45$. The predicted radii of massive hypernuclear stars are in the range of 13 km and are typically larger than the radii of their purely nucleonic counterparts.

Fig. 4 shows the parameter space covered by the coupling constants $x_{\sigma\Sigma}$ and $x_{\sigma\Lambda}$. The shaded (blue online) area is the parameter space consistent with Eq. (3). The dot corresponds to the values of these parameters predicted by the Nijmegen Soft Core (NSC) potential. The dashed (red online) line shows the optimal value of $x_{\sigma\Lambda}$ implied by the hypernuclear data. The solid vertical and horizontal lines show the parameter space explored in Ref. [17]. Finally, the square in the inset shows the maximal value of $x_{\sigma\Sigma} \simeq 0.45$ (at fixed $x_{\sigma\Lambda}$) which is still consistent with the $2M_\odot$ maximum value of a configuration. Thus, we conclude that the optimal values of the parameters correspond to

$$x_{\sigma\Lambda} = 0.6164, \qquad 0.15 \leq x_{\sigma\Sigma} \leq 0.45. \tag{8}$$

The first value is set by the study of (heavy) hypernuclei, the upper limit of the second value is set by the $2M_\odot$ constraint, whereas the lower limit is set by the requirement of the consistency with inequality (3).

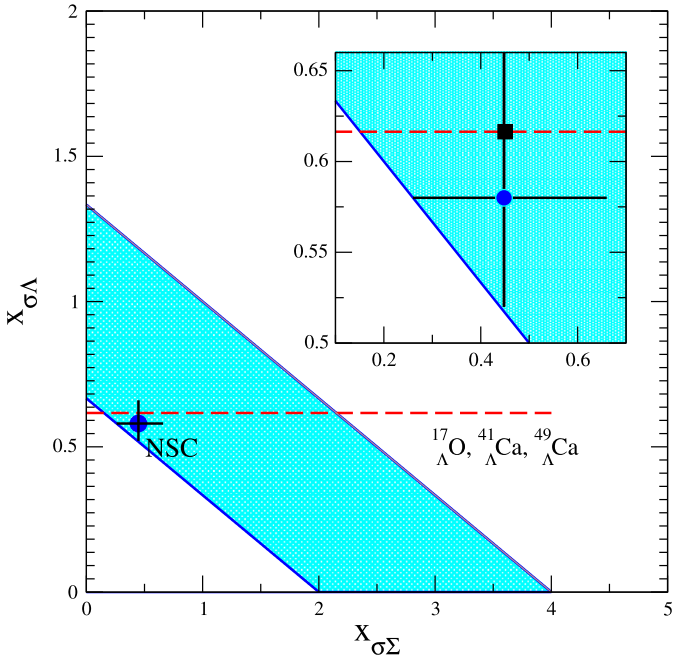

Fig. 4. (Color online.) The parameter space spanned by $x_{\sigma\Lambda}$ and $x_{\sigma\Sigma}$, where the inset enlarges the physically relevant area. The shaded (blue online) area corresponds to the inequality (3). The dot corresponds to the values $x_{\sigma\Lambda} = 0.58$ and $x_{\sigma\Sigma} = 0.448$ derived from the Nijmegen Soft Core (NSC) potential. The dashed (red online) line shows the best fit value of $x_{\sigma\Lambda} = 0.6164$ derived from hypernuclei. The square in the inset shows the limiting value of $x_{\sigma\Sigma} = 0.45$ for fixed $x_{\sigma\Lambda} = 0.6164$ beyond which no stars with $2M_\odot$ exist.

5. Conclusions

In this work we used a relativistic density functional theory of hypernuclear matter to extract bounds on the density-dependent couplings of a hypernuclear DFT. To do so, we used simultaneous fits to the medium-heavy Λ-hypernuclei and the requirement that the maximum mass of a hyperonic compact star is at least two-solar masses. This allowed us to narrow down significantly the parameter space of couplings of DFT – the range of optimal

values of parameters is given in Eq. (8). While our work was carried out within a specific parameterization of the hypernuclear density functional, it provides a proof-of-principle of the method for constraining any theoretical framework that describes hypernuclear systems using current laboratory and astrophysical data.

Acknowledgements

We are grateful to I. Mishustin, H. Müther, C. Providencia, L. Rezzolla, D. Rischke, and J. Schaffner-Bielich for discussions. This work was supported by a grant (Mu 705/7-1) of the Deutsche Forschungsgemeinschaft (E.N.E.v.D.), the HGS-HIRe graduate program at Frankfurt University (G.C.) and by "NewCompStar", COST Action MP1304.

References

[1] P.B. Demorest, T. Pennucci, S.M. Ransom, M.S.E. Roberts, J.W.T. Hessels, A two-solar-mass neutron star measured using Shapiro delay, Nature 467 (2010) 1081–1083.
[2] J. Antoniadis, et al., A massive pulsar in a compact relativistic binary, Science 340 (2013) 448.
[3] E. Engel, R.M. Dreizler, Density Functional Theory, Springer, New York, 2013.
[4] F. Weber, Pulsars as Astrophysical Laboratories for Nuclear and Particle Physics, Institute of Physics, Bristol, 1999.
[5] A. Sedrakian, The physics of dense hadronic matter and compact stars, Prog. Part. Nucl. Phys. 58 (2007) 168–246.
[6] C.-Y. Ryu, C.H. Hyun, C.-H. Lee, Hyperons and nuclear symmetry energy in neutron star matter, Phys. Rev. C 84 (2011) 035809.
[7] R. Lastowiecki, D. Blaschke, H. Grigorian, S. Typel, Strangeness in the cores of neutron stars, Acta Phys. Pol. B, Proc. Suppl. 5 (2012) 535–540.
[8] S. Weissenborn, D. Chatterjee, J. Schaffner-Bielich, Hyperons and massive neutron stars: vector repulsion and SU(3) symmetry, Phys. Rev. C 85 (2012) 065802;
S. Weissenborn, D. Chatterjee, J. Schaffner-Bielich, Hyperons and massive neutron stars: the role of hyperon potentials, Nucl. Phys. A 881 (2012) 62–77.
[9] L. Bonanno, A. Sedrakian, Composition and stability of hybrid stars with hyperons and quark color-superconductivity, Astron. Astrophys. 539 (2012) A16.
[10] I. Bednarek, P. Haensel, J.L. Zdunik, M. Bejger, R. Mańka, Hyperons in neutron-star cores and a $2M_{\odot}$ pulsar, Astron. Astrophys. 543 (2012) A157.
[11] É. Massot, J. Margueron, G. Chanfray, On the maximum mass of hyperonic neutron stars, Europhys. Lett. 97 (2012) 39002.
[12] C. Providência, A. Rabhi, Interplay between the symmetry energy and the strangeness content of neutron stars, Phys. Rev. C 87 (2013) 055801.
[13] N. Chamel, P. Haensel, J.L. Zdunik, A.F. Fantina, On the maximum mass of neutron stars, Int. J. Mod. Phys. E 22 (2013) 30018.
[14] V. Dexheimer, J. Steinheimer, R. Negreiros, S. Schramm, Hybrid stars in an SU(3) parity doublet model, Phys. Rev. C 87 (2013) 015804.
[15] N.K. Glendenning, S.A. Moszkowski, Reconciliation of neutron-star masses and binding of the Λ in hypernuclei, Phys. Rev. Lett. 67 (1991) 2414–2417.
[16] G.A. Lalazissis, T. Nikšić, D. Vretenar, P. Ring, New relativistic mean-field interaction with density-dependent meson–nucleon couplings, Phys. Rev. C 71 (2005) 024312.
[17] G. Colucci, A. Sedrakian, Equation of state of hypernuclear matter: impact of hyperon–scalar-meson couplings, Phys. Rev. C 87 (2013) 055806.
[18] C. Ducoin, J. Margueron, C. Providência, I. Vidaña, Core-crust transition in neutron stars: predictivity of density developments, Phys. Rev. C 83 (2011) 045810.
[19] A. Krasznahorkay, et al., Neutron-skin thickness of ^{208}Pb, and symmetry-energy constraints from the study of the anti-analog giant dipole resonance, arXiv:1311.1456, 2013.
[20] C. Fuchs, H. Lenske, H.H. Wolter, Density dependent hadron field theory, Phys. Rev. C 52 (1995) 3043–3060.
[21] S. Typel, H.H. Wolter, Relativistic mean field calculations with density-dependent meson–nucleon coupling, Nucl. Phys. A 656 (1999) 331–364.
[22] KLOE Collaboration, F. Ambrosino, et al., A global fit to determine the pseudoscalar mixing angle and the gluonium content of the η' meson, J. High Energy Phys. 7 (2009) 105.
[23] J.J. de Swart, The octet model and its Clebsch–Gordan coefficients, Rev. Mod. Phys. 35 (1963) 916–939.
[24] M. Rufa, J. Schaffner, J. Maruhn, H. Stöcker, W. Greiner, P.-G. Reinhard, Multi-lambda hypernuclei and the equation of state of hypermatter, Phys. Rev. C 42 (1990) 2469–2478.
[25] C.M. Keil, F. Hofmann, H. Lenske, Density dependent hadron field theory for hypernuclei, Phys. Rev. C 61 (2000) 064309.
[26] P. Finelli, N. Kaiser, D. Vretenar, W. Weise, Hypernuclear single particle spectra based on in-medium chiral SU(3) dynamics, Nucl. Phys. A 831 (2009) 163–183.
[27] F. Montani, C. May, H. Müther, Mean field and pairing properties in the crust of neutron stars, Phys. Rev. C 69 (2004) 065801.
[28] E.N.E. van Dalen, P. Gögelein, H. Müther, Bulk properties of nuclei and realistic NN interactions, Phys. Rev. C 80 (2009) 044312.
[29] G. Lévai, J. Cseh, P. van Isacker, O. Juillet, Mass formula for Λ hypernuclei based on SU(6) symmetry, Phys. Lett. B 433 (1998) 250–256.
[30] G. Erkol, R.G.E. Timmermans, M. Oka, T.A. Rijken, Scalar-meson–baryon coupling constants in QCD sum rules, Phys. Rev. C 73 (2006) 044009.